

Angular and Velocity Distributions Characteristic of the Transition between the Thermal and Structure Regimes of Gas-Surface Scattering

C. T. Rettner, J. A. Barker, and D. S. Bethune

IBM Almaden Research Center, K33/801, 650 Harry Road, San Jose, California 95120-6099

(Received 6 May 1991)

Angular variations in the kinetic energy of scattered species are found to provide a useful probe of the transition between gas-surface scattering regimes, complementing angular flux distributions. As incidence energies exceed a few eV, these change from being consistent with scattering from an extended target to being more typical of scattering from individual atoms. Results are presented for the Xe/Pt(111) system and are supported by detailed trajectory calculations.

PACS numbers: 79.20.Rf

An understanding of the dynamics of energy transfer at the gas-surface interface is required for detailed modeling of many different chemical and physical phenomena associated with this interface. These range from the trapping and sticking of atoms and molecules at relatively low energies [1], to sputtering, plasma etching, and implantation at hyperthermal energies [2]. Such knowledge is also of value in the design of spacecraft [3] and thermonuclear fusion reactors [4]. Molecular-beam scattering techniques offer a powerful tool for probing such interactions and have been employed to examine many different systems. However, most studies have concerned angular distributions of scattered species for relatively low incidence energies, providing only a limited picture of the scattering dynamics. Since angular distributions reflect both the static corrugation of the gas-surface potential and differential momentum transfer parallel and perpendicular to the surface, velocity measurements are required for unambiguous interpretation. While high-energy collisions have been recognized as qualitatively distinct from those at low energy for many years [5–12], there is little experimental data that directly relate to the transition between these regimes.

In this Letter we report results for the scattering of Xe from Pt(111) which clearly show that variations in the energies of scattered species with scattering angle can be used to characterize the degree of penetration. At low incidence energies, $E_i < 1$ eV, we find that the energies after scattering, E_f , decrease with increasing scattering angle θ_f in a manner approximately consistent with parallel momentum conservation. At high energies, $E_i > 5$ eV, the opposite trend is observed, with E_f increasing with increasing final angle, in a manner consistent with scattering from one or more individual surface atoms. These qualitative conclusions are supported by detailed trajectory calculations.

The molecular-beam surface scattering apparatus and the experimental techniques appropriate to this study have been described elsewhere [12–14]. The mounting of the Pt(111) crystal is such that the scattering plane intercepts the (111) face close to the $[1\bar{2}1]$ azimuth. Contamination levels are below our Auger detection limits (1%), sharp LEED patterns are obtained, and He scattering gives a specular peak width indistinguishable from the in-

strumental resolution of 1.6° . The energies of incident and scattered atoms are determined from their flight times between a high-speed chopper and the differentially pumped mass spectrometer which can rotate about the same axis as the crystal [13].

We have determined the angular and velocity distributions of Xe scattering from Pt(111) over a wide range of conditions, varying the incidence energy from ~ 0.1 eV to over 14 eV and the incidence angle from 15° to 60° . Most measurements have been made at a surface temperature T_s of 800 K. Figure 1 displays typical scattering data, obtained with $E_i = 1.17$ eV and $\theta_i = 30^\circ$. Intensities correspond to the flux at a given angle. Mean energies are also indicated for a range of scattering angles, and can be compared with the overall mean energy averaged over all final angles. Figures 2 and 3 display similar data for $E_i = 0.52$ eV and $E_i = 6.8$ eV, respectively.

The width and shape of the angular distributions are found to vary systematically with incidence energy and

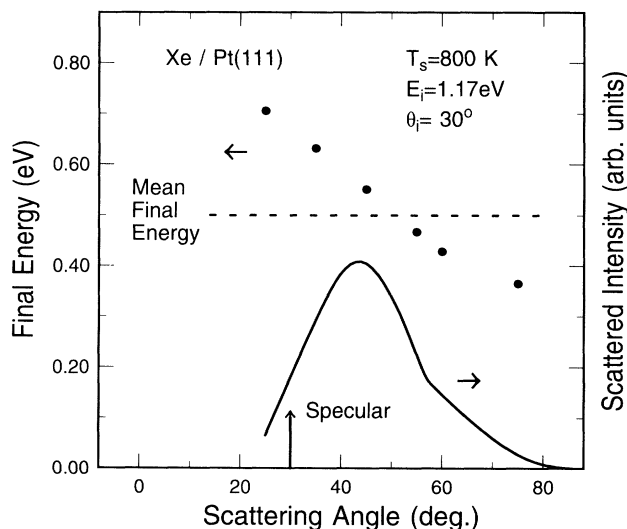


FIG. 1. Intensities and mean final translational energies of Xe atoms scattered from Pt(111) at different final angles. Here the incidence energy was 1.17 eV, the incidence angle 30° with respect to the surface normal, and the surface temperature 800 K.

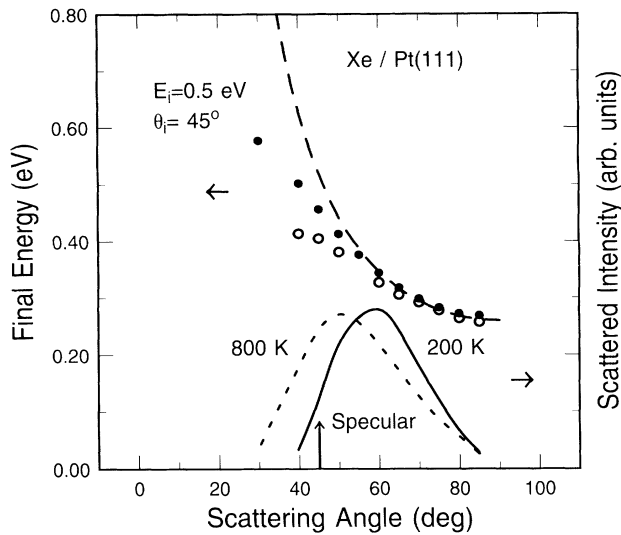


FIG. 2. Same as Fig. 1 but for $E_i=0.5$ eV and $\theta_i=45^\circ$. Results are displayed for surface temperatures of 800 K (dotted line, solid symbols) and 200 K (solid line, open symbols). The dashed line indicates the behavior expected for strict parallel momentum conservation.

angle. At the lowest energies, ~ 0.1 eV, a distinct trapping-desorption component [1,15] is discernible, while at energies above about 6 eV, distributions show structure suggestive of surface rainbow scattering [16]. These trends are summarized in Fig. 4, which displays the angular widths (FWHM) as a function of E_i for $\theta_i=30^\circ, 45^\circ$, and 60° . The results are consistent with previous scattering studies [6,7,9-12], and calculations [5], and can be said to cover the transition from the so-called "thermal scattering" regime at low energies to the "structure scattering" regime at high energies.

We find that the measured differential energy distributions provide considerable additional insight into the dynamics of the scattering under the extreme high- and low-energy conditions and of the transition between them. At low energy, for $E_i \lesssim 1$ eV, we observe that E_f increases rapidly with decreasing θ_f . In contrast, at high energy, for $E_i \gtrsim 6$ eV, E_f is found to rise with increasing θ_f . The behavior for a range of incidence energies with $\theta_i=45^\circ$ is indicated in Fig. 5. It is apparent that the slopes of these plots vary smoothly with increasing E_i , passing through zero slope at an energy of about 2 eV and continuing to increase up to the highest energy studied. Note the energy of 2 eV also yields the narrowest angular distribution at $\theta_i=45^\circ$ (see Fig. 4). An interesting aspect of the data is that all plots converge on a mean fractional energy loss close to 0.5 at $\theta_f=90^\circ$. Results for $\theta_i=30^\circ$ and 60° are qualitatively similar, but the corresponding plots converge on fractional energy losses of 0.25 and 0.65, respectively.

The narrowing of the angular distributions with increasing energy at low energy is qualitatively consistent with the predictions of a simple hard-cube model [17,18],

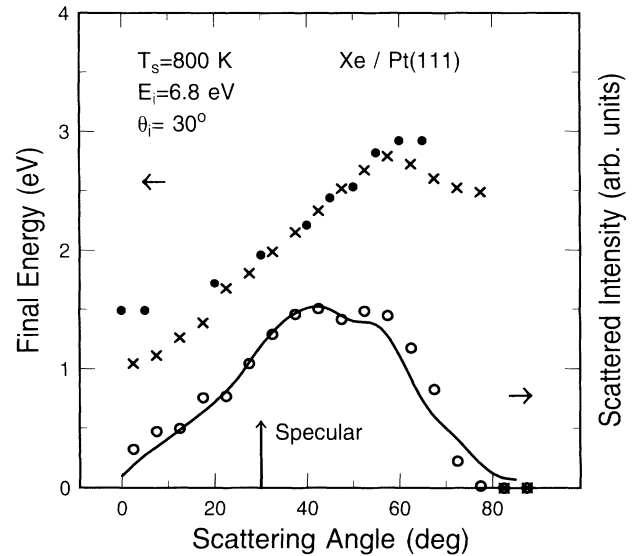


FIG. 3. Same as Fig. 1 but for $E_i=6.8$ eV and $\theta_i=30^\circ$. The experimental results are shown as the solid curve and the solid circles. Calculated intensities and mean energies are displayed as open circles and crosses, respectively.

in which parallel momentum is conserved in the scattering process. Here the angular width reflects the range of normal momentum transfer associated with different cube velocities. Thus scattering to angles smaller than the specular follows collisions in which the cube is moving "outwards," which increases the collision energy. The spread in cube velocities then becomes less important as

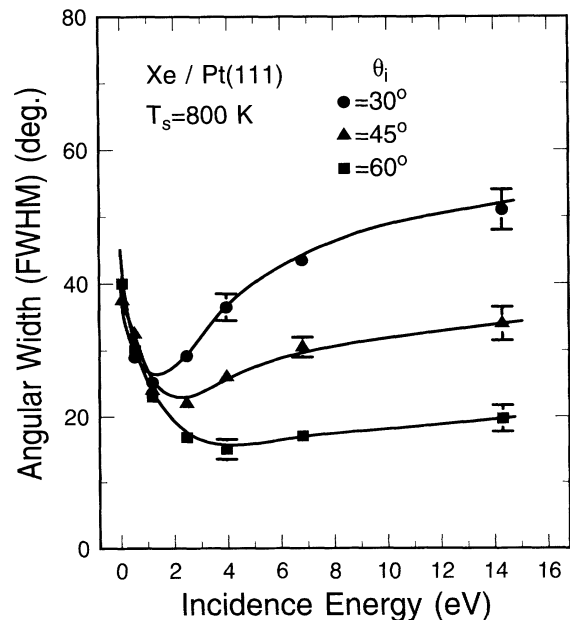


FIG. 4. Variation of the widths (FWHM) of angular distributions for Xe scattering from Pt(111) at a surface temperature of 800 K for incidence angles of $30^\circ, 45^\circ$, and 60° .

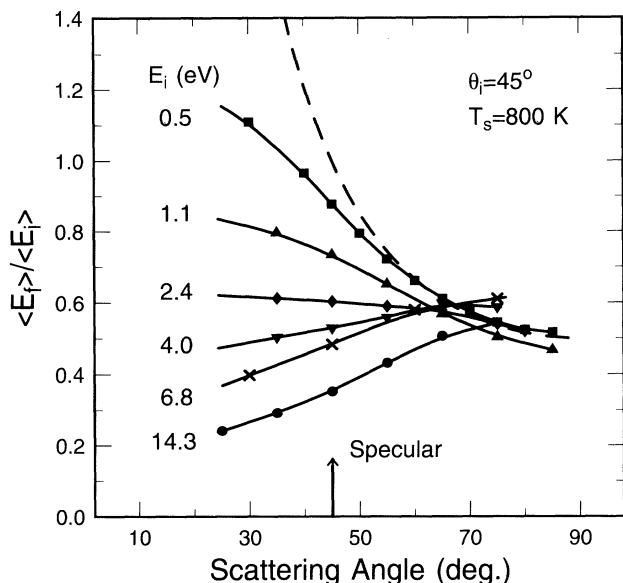


FIG. 5. Variation of the mean final energy with scattering angle for Xe scattering from Pt(111) at a surface temperature of 800 K for an incidence angle of 45° . Energies are normalized to the mean incidence energy which is indicated for each curve. The dashed line indicates the behavior expected for strict parallel momentum conservation.

E_i increases. The degree of parallel momentum conservation can be tested more directly by determination of the differential momenta of the scattered species. Strict parallel momentum conservation requires that $E_f/E_i = (\sin\theta_i/\sin\theta_f)^2$, for each final angle. This relationship is indicated as a dashed line in Figs. 2 and 5. It is apparent that results do indeed roughly follow this prediction at the lowest E_i 's, particularly for scattering at angles larger than specular. Again, identical trends are found for incidence angles of 30° and 60° . In keeping with this model, the actual fluxes at a given angle are strongly dependent on T_s , for low E_i . This is apparent from Fig. 2 which shows that there is very little subspecular intensity for $T_s = 200$ K, so that the angular width is narrower than at 800 K. Changing T_s is seen to have very little effect on $\langle E_f \rangle$.

The increase in angular widths at high E_i , evident from Fig. 4, suggests that the scattering is qualitatively different under these conditions. It is clear from Figs. 4 and 5 that the angular variations in E_f are also completely different from the parallel-momentum-conservation case. The trend observed at the highest energy of 14.3 eV is completely reversed, with the lowest energies occurring at small scattering angles. This behavior is closer to that expected for hard-sphere scattering, in which the energy lost by an incident particle grows as the total deflection angle increases. A similar trend in differential energies has been reported recently by Spruit *et al.* for O_2 scattering from Ag(111) with $E_i = 1.5$ eV [10]. In this case relatively broad angular distributions are also observed and

essentially the same interpretation has been given. In one respect we find that scattering at low and high energies are similar. Just as for the low-energy case, we observe that angular distributions for high incidence energies are somewhat sensitive to T_s , but that mean final energies are relatively insensitive to this parameter for a given final angle. For example, the slight dip in the intensity distribution of Fig. 3 becomes much more pronounced at 400 K, but the mean energies at a given final angle are virtually unchanged from the 800-K measurements.

Clearly the gas-surface situation is more complex than hard-sphere scattering. We have thus performed classical trajectory calculations to examine this question further. We have developed a detailed potential which is able to account for results over the full range of energies studied, details of which will be reported elsewhere [19]. Our calculations suggest that the tendency towards parallel momentum conservation at low energies arises because the interaction with conduction electrons is relatively independent of the position in the unit-cell position—so that the surface appears relatively flat. In addition, the turning point on our potential is sufficiently far from the ion cores that the incident atoms interact with many surface atoms—again giving rise to a relatively flat interaction.

At higher energies, the incident atoms penetrate beyond these relatively soft regions of the potential and sample the steep repulsive interactions with the individual ion cores. The dynamics in this region can be adequately accounted for using a much simpler interaction potential. We have therefore carried out calculations based on a much simplified potential consisting of a sum of pair interactions between the Xe atom and each Pt atom, having the simple repulsive exponential form $u(R) = A \exp(-\alpha R)$, together with a harmonic interaction between nearest-neighbor Pt atoms with force constant 4.56×10^4 erg cm $^{-2}$. The calculations used standard molecular-dynamics methods with a 6×6 surface of four layers with periodic boundary conditions parallel to the surface. The surface temperature was maintained at 800 K by scaling the velocities at each time step. The high-energy scattering results can be reproduced using $A = 4.65 \times 10^6$ eV and $\alpha = 6.5 \text{ \AA}^{-1}$. A calculated in-plane angular distribution has been added to the experimental results of Fig. 3, together with calculated mean final energies. It is seen that good agreement is obtained. These calculations also qualitatively reproduce the observed dependence on T_s , which is the subject of ongoing studies.

Analysis of these computations reveals that trajectories which lead to in-plane scattering have classical turning points concentrated along a line parallel to the [121] direction and passing through the atom centers. It is therefore useful to look at the energy transfer as a function of position along this line. The result is displayed in Fig. 6 for the conditions of Fig. 3 ($E_i = 6.8$ eV, $\theta_i = 30^\circ$). Here we plot the final energy of the scattered Xe against the position of the turning point, or impact parameter,

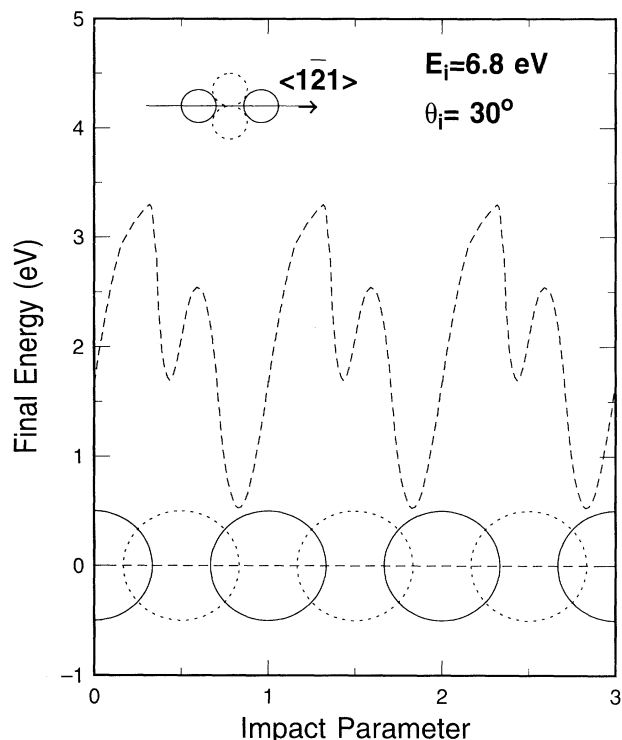


FIG. 6. Calculated mean final energy as a function of the impact point along a line parallel to the $[1\bar{2}1]$ direction and passing through the atom centers (see inset). These results refer to the conditions of Fig. 3, $E_i = 6.8$ eV and $\theta_i = 30^\circ$. Integral-value impact parameters correspond to collisions directly on top of an atom, as indicated by the large solid circles. The dashed circles indicate the projection of the atoms placed on either side of this line (aligned parallel to the $[10\bar{1}]$ direction).

along this direction. It is seen that the lowest final energies are associated with collisions just in front of the on-top position. We find that the atoms are scattered close to the normal in this case. At the other extreme, the highest final energies are associated with collisions just beyond the on-top position. These atoms scatter to grazing angles. This behavior is indeed close to what one might expect for hard-sphere collisions. However, collisions at positions between two on-top sites cannot be described in terms of single impacts. Here the incident atom interacts with several surface atoms and scatters at about 45° to the normal. Note that the second maximum in the final energy occurs for collisions just past the centers of the two atoms which lie to either side of the line (dashed atoms in inset of Fig. 6).

Both the experiments and the calculations indicate that the gas-surface collisions are very inelastic at high incidence energies. The angular distributions are thus strongly influenced both by the energy exchange and by transfer between normal and parallel momentum associated with the corrugation. The name "structure scatter-

ing," if it is interpreted to mean that the corrugation is dominant, is thus an oversimplification of this relatively complex behavior.

In summary, we have presented scattering data for the Xe/Pt(111) system covering a wide range of energies. We have shown that the scattering is qualitatively different at high and low energies and have demonstrated that measurements of the mean energies of scattered atoms provide useful insight into the scattering dynamics at a given energy.

We thank E. K. Schweizer and J. E. Schlaegel for technical assistance, and D. J. Auerbach for useful discussions.

- [1] J. A. Barker and D. J. Auerbach, *Surf. Sci. Rep.* **4**, 1 (1984).
- [2] H. F. Winters, H. Coufal, C. T. Rettner, and D. S. Bethune, *Phys. Rev. A* **41**, 6240 (1990).
- [3] F. C. Hurlbut, *Prog. Astronaut. Aeronaut.* **116**, 419 (1989).
- [4] R. Ito, T. Tabata, N. Itoh, K. Morita, T. Kafo, and H. Tawara, The Institute of Plasma Physics, Nagoya University, Japan, Report No. IPPJ-AM-41, 1985 (unpublished).
- [5] R. A. Oman, *J. Chem. Phys.* **48**, 3919 (1968).
- [6] D. R. Miller and R. B. Subbarao, *J. Chem. Phys.* **52**, 425 (1970).
- [7] S. M. Lui, W. E. Rodgers, and E. L. Knuth, in *Proceedings of the Ninth International Symposium on Rarefied Gas Dynamics* (Deutsche Forschungs- und Versuchsanstalt für Luft- und Raumfahrt, Porz-Wahn, Germany, 1974), Vol. II, p. E.8-1.
- [8] A. Amirav, M. J. Cardillo, P. L. Trevor, C. Lim, and J. C. Tully, *J. Chem. Phys.* **87**, 1796 (1987).
- [9] C. T. Rettner and E. K. Schweizer, *Surf. Sci.* **203**, L677 (1988).
- [10] M. E. Spruit, P. J. van den Hoek, E. W. Kuipers, F. H. Geuzebroek, and A. W. Kleyn, *Phys. Rev. B* **39**, 3915 (1989).
- [11] M. E. Spruit, P. J. van den Hoek, E. W. Kuipers, F. H. Geuzebroek, and A. W. Kleyn, *Surf. Sci.* **214**, 591 (1989).
- [12] C. T. Rettner, E. K. Schweizer, and H. Stein, *J. Chem. Phys.* **93**, 1442 (1990).
- [13] C. T. Rettner, L. A. DeLouise, and D. J. Auerbach, *J. Chem. Phys.* **85**, 1131 (1986).
- [14] C. T. Rettner, H. Stein, and E. K. Schweizer, *J. Chem. Phys.* **89**, 3337 (1988).
- [15] J. E. Hurst, C. A. Becker, J. P. Cowin, K. C. Janda, L. Wharton, and D. J. Auerbach, *Phys. Rev. Lett.* **43**, 1175 (1979).
- [16] See, for example, A. W. Kleyn and T. C. M. Horn, *Phys. Rep.* **199**, 191 (1991).
- [17] R. M. Logan and R. E. Stickney, *J. Chem. Phys.* **44**, 195 (1966).
- [18] E. K. Grimmelmann, J. C. Tully, and M. J. Cardillo, *J. Chem. Phys.* **72**, 1039 (1980).
- [19] J. A. Barker, C. T. Rettner, and D. S. Bethune (to be published).